ACTA IMEKO
ISSN: 2221-870X
September 2026, Volume 15, Number 3, 1 – 7

Dynamic and quasi-static characterization and Cowper–Symonds material model calibration of photopolymer resins produced by stereolithography

Tomáš Doktor[1], Veronika Drechslerová[1], Jan Falta[1], Tomáš Fíla[1], Václav Rada[2], Bohumil Hora[1], Daniel Kytýř[2], Petr Koudelka[1]

[1] *Czech Technical University in Prague, Faculty of Transportation Sciences*
[2] *Czech Academy of Sciences, Institute of Theoretical and Applied Mechanics*

ABSTRACT
Photopolymer resins produced by stereolithography (SLA) are widely used for manufacturing lattice structures and mechanical metamaterials intended for experimental validation of numerically designed structures. Reliable simulations of their response under dynamic loading require constitutive models capable of describing strain-rate-dependent material behavior; however, suitable experimental data for commercially available SLA resins remain limited. This study presents the experimental characterization and Cowper–Symonds model calibration of two SLA printing materials: Phrozen Aqua Blue Resin and Phrozen High-Resolution RPG Resin. Cylindrical bulk specimens were manufactured by SLA and tested under quasi-static compression and high-strain-rate compression using a split Hopkinson pressure bar apparatus. The resulting stress–strain curves were used to evaluate the strain-rate sensitivity of both resins. Yield stress values determined at different strain rates served as input data for the calibration of the Cowper–Symonds parameters. The calibrated material parameters are intended for implementation in LS-DYNA together with the quasi-static material response, for explicit simulations of dynamically loaded SLA-printed structures. The results provide experimentally derived material data for future numerical simulations of SLA-printed lattice structures and mechanical metamaterials.

Section: RESEARCH PAPER

Keywords: SLA-printed resins; split Hopkinson pressure bar; strain-rate sensitivity; Cowper–Symonds material model

Citation: T. Doktor, V. Drechslerová, J. Falta, T. Fíla, V. Rada, B. Hora, D. Kytýř, P. Koudelka, Dynamic and quasi-static characterization and Cowper–Symonds material model calibration of photopolymer resins produced by stereolithography, Acta IMEKO, vol. 15 (2026) no. 3, pp. 1–7. DOI: 10.21014/actaimeko.v15i3.2485

Section Editor: Emina Hadzalic, University of Rijeka, Croatia

Received: August 10, 2026; **In Final Form:** August 28, 2026; **Published:** September, 2026.

Funding: This research was supported by the Czech Science Foundation (Project No. 25-18209S), the Strategy AV21 programme “AI: Artificial Intelligence for Science and Society”.

Corresponding Author: Tomáš Doktor, e-mail: tomas.doktor@cvut.cz

1. INTRODUCTION

Additive manufacturing has become an important tool for the fabrication, optimization, and experimental validation of lattice structures and mechanical metamaterials. Structures based on re-entrant, chiral, honeycomb, or other architectured topologies can exhibit tailored mechanical properties, including auxetic deformation, enhanced compliance, controlled collapse, and improved strain energy absorption [1]–[3]. Since the design space of such structures is very large, their development is commonly driven by numerical optimization and finite element simulations [4]. Nevertheless, physical experiments remain essential for assessing the predicted deformation mechanisms, failure modes, and energy absorption capabilities, especially when the structures are intended for dynamic or impact-related applications [5]–[7].

For this purpose, polymer additive manufacturing offers an accessible route for producing specimens for experimental validation with complex geometries at relatively low cost and with short production times. In particular, stereolithography (SLA) and related photopolymerization techniques provide high geometrical accuracy and good surface quality, which are advantageous for small lattice specimens and mechanical metamaterials with thin struts and fine structural details. Compared with powder-based additive manufacturing routes, such as selective laser sintering or metal laser powder bed fusion, SLA printing can serve as a fast and accessible experimental platform for preliminary validation of optimized structural concepts [8].

However, the use of SLA-printed specimens for the validation of dynamically loaded structures requires reliable knowledge of the mechanical response of the base photopolymer resin. The mechanical behavior of printed polymers can be affected by the printing parameters, post-curing conditions, loading mode, and strain rate. Although quasi-static material data are often available from manufacturer datasheets or standard mechanical tests, high-strain-rate data suitable for numerical model calibration are much less common. Neglecting the strain-rate dependence of the base material in simulations of impact or rapid compression may therefore lead to inaccurate predictions of the structural response, including deformation mechanisms, peak forces, and absorbed energy [9]–[12].

A convenient engineering approach to include strain-rate sensitivity in explicit dynamic simulations is the Cowper-Symonds model [13]. In this model, the flow stress is scaled according to the current strain rate using two material parameters, which can be calibrated from experimentally determined yield stress values at different strain rates. The model is simple, computationally inexpensive, and directly available in commonly used explicit finite element codes. Although it does not provide a comprehensive constitutive description of the rate-dependent behavior of photopolymer materials, it offers a practical phenomenological approach for incorporating the experimentally observed increase in flow stress with strain rate into numerical simulations.

This work focuses on the experimental characterization of the strain-rate-dependent compressive behavior of commercially available SLA-printed photopolymer resins and the identification of parameters for their constitutive modeling. Bulk cylindrical specimens were tested in compression under quasi-static and elevated strain-rate conditions, the latter using a split Hopkinson pressure bar apparatus. The obtained stress–strain curves were used to evaluate the strain-rate sensitivity of the tested materials and to calibrate the parameters of the Cowper–Symonds model. The resulting experimental data and calibrated material parameters are intended for future explicit dynamic simulations of SLA-printed lattice structures and mechanical metamaterials.

2. MATERIALS AND METHODS

2.1. Specimen geometry and manufacturing

Two commercially available photopolymer resins compatible with SLA 3D printing were investigated: Phrozen Aqua Blue Resin and Phrozen High-Resolution RPG Resin (Phrozen, Taiwan). The specimens were manufactured using a Sonic Mighty 4K printer (Phrozen, Taiwan).

The cylindrical specimen geometry was used for both quasi-static compression tests and split Hopkinson pressure bar (SHPB) experiments. All the specimens had a nominal diameter of $D = 12$ mm and a nominal height of $h = 12$ mm. The specimens were printed with a layer height of 50 μm. The use of identical geometry for both loading regimes enabled a direct comparison between quasi-static and dynamic compression response, and simplified the subsequent evaluation of strain-rate-dependent material parameters.

After printing, the specimens were rinsed with water and cleaned in an isopropyl alcohol ultrasonic bath for 5 min at 35 °C. The cleaned specimens were subsequently post-cured using a Cure Luna UV curing unit (Phrozen, Taiwan). Following UV post-curing, all specimen batches were stored for one week prior to testing to allow their mechanical properties to stabilize [8].

2.2. Quasi-static compression testing

Quasi-static compression tests were performed using an Instron 3382 (Instron, USA) universal uniaxial testing machine under displacement control. For each investigated resin, five specimens were tested.

The specimens were compressed at a crosshead displacement rate of 1 mm/min, corresponding to an initial engineering strain rate of approximately 1.39×10^{-3} s^{-1}. The deformation was then evaluated from the crosshead displacement. The tests were performed under dry contact conditions between the specimen and the compression platens. No additional lubrication or surface treatment was used, as the planparallelism of the SLA-printed cylindrical specimens was sufficient for a stable compression loading.

The acquired force–displacement curves were converted to engineering stress–strain response using the initial specimen dimensions. Engineering strain was calculated from the crosshead displacement and the initial specimen height, while engineering stress was calculated from the measured force and the initial cross-sectional area. The engineering quantities were subsequently converted to true stress and true strain according to Equations 1 and 2.

$$\varepsilon_{\mathrm{true}} = -\ln\left(1 - \varepsilon_{\mathrm{eng}}\right) \tag{1}$$

$$\sigma_{\mathrm{true}} = \sigma_{\mathrm{eng}}\left(1 - \varepsilon_{\mathrm{eng}}\right) \tag{2}$$

2.3. Split Hopkinson pressure bar testing

Dynamic compression experiments were performed using an in-house split Hopkinson pressure bar (SHPB) apparatus [14] based on Kolsky setup [15]. The experimental setup is depicted in Figure 1. The same cylindrical specimen geometry as in the quasi-static experiments was used. For each investigated resin, five specimens were tested at each of the two dynamic loading levels.

The SHPB apparatus consisted of aluminium incident and transmission bars, both 3000 mm in length and 30 mm in diameter. An aluminium striker with a length of 2700 mm and a diameter of 30 mm was used to generate the loading pulse. The strain-gauge signals were recorded with a sampling frequency of 1 MHz. Two loading configurations were used to obtain different strain-rate levels. The lower strain-rate configuration was achieved using a striker pressure of 3.5 bar and a copper pulse shaper with dimensions of 15 mm (diameter) × 0.5 mm. The higher strain-rate configuration used a striker pressure of 9.5 bar and a copper pulse shaper with dimensions of 8 mm (diameter) × 0.5 mm. The resulting strain rates were evaluated individually from the measured signals and are reported in the Results section.

2.4. SHPB setup verification

Before the material tests, the SHPB setup and signal-processing procedure were verified using a void test performed without a specimen between the bars. The forces and particle velocities reconstructed from the incident and transmission bars were compared. The agreement of the reconstructed signals confirmed proper synchronization of the strain-gauge channels and consistency of the signal-processing procedure used for the subsequent SHPB experiments.

2.5. Data processing

The recorded incident, reflected, and transmitted strain waves were used to evaluate the specimen stress, strain, and strain-rate histories [16]. The resulting stress–strain and strain-rate–strain curves were then used for the identification of yield stress values at different strain rates. These values served as input data for the subsequent calibration of the strain-rate-dependent constitutive model. The dynamic force equilibrium during the SHPB experiments, which serves as a criterion of the test validity, was assessed by comparing the forces acting at the incident bar–specimen and

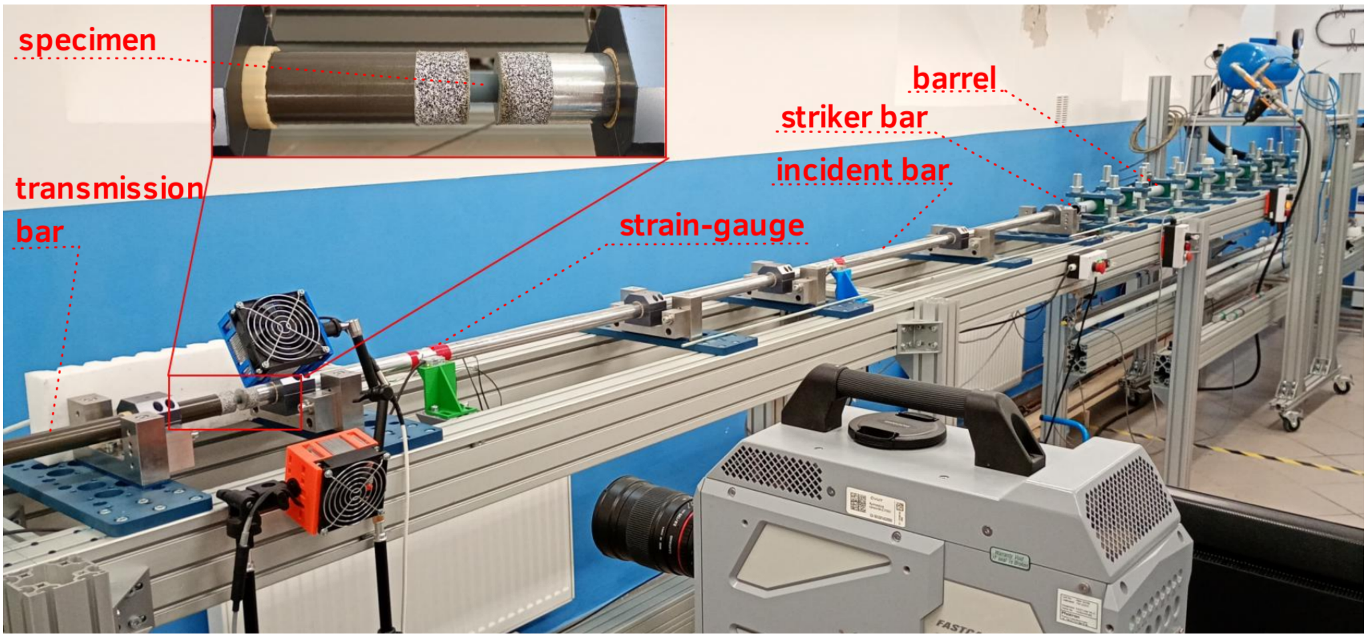

Figure 1. In-house split Hopkinson pressure bar (SHPB) setup used for dynamic compression testing, showing the striker, incident and transmission bars, strain-gauge location, and specimen positioned between the bars.

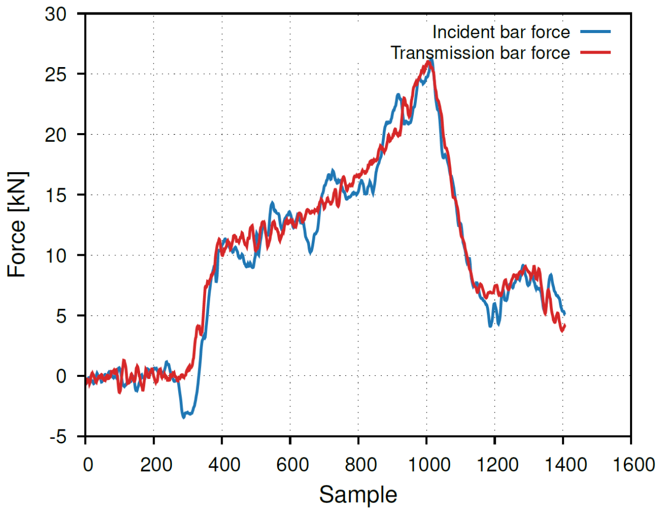

Figure 2. Example of the force equilibrium during the SHPB loading test.

specimen–transmission bar interfaces. A representative example of this comparison is shown in Figure 2.

2.6. Cowper–Symonds model calibration

The strain-rate sensitivity of the investigated SLA-printed resins was described using the Cowper–Symonds model. In this model, the dynamic yield stress is expressed as a function of strain rate according to Equation 3 where $\sigma_y(\dot{\varepsilon})$ is the strain-rate-dependent yield stress, σ_0 is the quasi-static reference yield stress, $\dot{\varepsilon}$ is the strain rate, and C and p are material parameters controlling the strain-rate sensitivity.

$$\sigma_y(\dot{\varepsilon}) = \sigma_0 \left[1 + \left(\frac{\dot{\varepsilon}}{C} \right)^{1/p} \right], \tag{3}$$

For each resin, the quasi-static compression tests were used to determine the reference yield stress σ_0, while the SHPB experiments provided the dynamic yield stress values at two elevated strain-rate levels. All yield stress values were determined from the processed true-stress–true-strain curves. The yield stress was manually identified as the stress corresponding to the onset of deviation from the initial, approximately linear portion of each true-stress–true-strain curve. The same criterion was applied consistently to all quasi-static and dynamic curves.

The experimentally determined strain-rate–yield-stress data, consisting of one quasi-static reference point (taken as the mean yield stress obtained from the quasi-static tests) and five strain-rate–yield-stress pairs for each of the two dynamic SHPB loading conditions, were subsequently used to calibrate the Cowper–Symonds parameters (C) and (p). The parameters were identified separately for each resin by fitting the model response to the experimental data using nonlinear least-squares optimization.

The calibrated parameter sets provide a compact engineering description of the strain-rate-dependent compressive response of the investigated SLA-printed resins. In future explicit finite element simulations, the quasi-static true-stress–true-strain response can be used as the reference material curve, while the Cowper–Symonds parameters scale the flow stress according to the local strain rate.

3. RESULTS

3.1. Quasi-static compression response

The quasi-static compression response of the Phrozen Standard Aqua Blue Resin and Phrozen High-Resolution RPG Resin is shown in Figures 3 and 4, respectively. For each material, five cylindrical specimens were tested under identical displacement-controlled loading conditions. The resulting true-stress–true-strain curves showed a consistent quasi-static response among the individual specimens and provide the reference material behavior for the subsequent strain-rate sensitivity evaluation.

The Aqua Blue resin exhibited a characteristic compressive response with an initially nearly linear region followed by a transition to plastic deformation, as shown in Figure 3. The solid curve represents the mean response, while the shaded band indicates the standard deviation calculated from repeated tests. The individual curves showed comparable shape and stress level, indicating a good

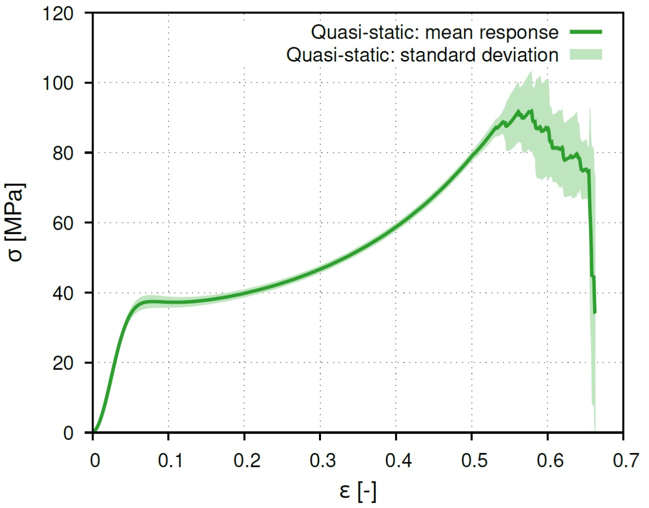

Figure 3. Quasi-static response of AquaBlue resin.

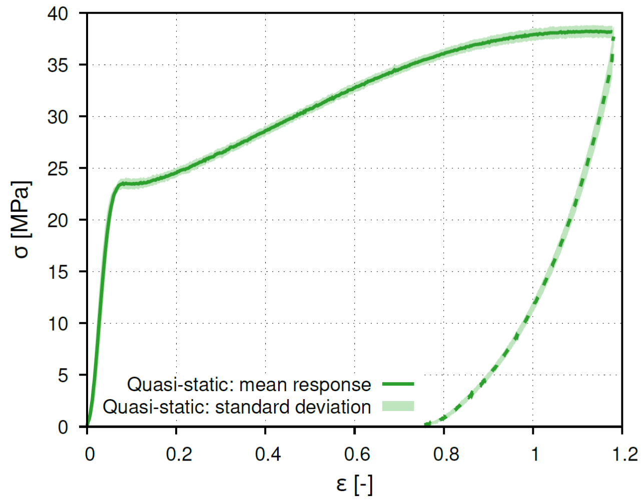

Figure 4. Quasi-static response of RPG resin.

repeatability of the measured quasi-static response. The manually selected yield points from the quasi-static curves were used to determine the reference yield stress σ_0 for the Cowper–Symonds calibration.

The RPG resin response is presented in Figure 4. Similarly, the solid curve shows the mean response and the shaded band represents the corresponding standard deviation. Compared with Aqua Blue resin, the RPG specimens showed a distinctly different true stress–true strain response, indicating differences in the compressive behavior of the two resin systems. The quasi-static RPG curves were processed using the same procedure as for Aqua Blue resin, and the corresponding yield stress values were used to determine the quasi-static reference yield stress for the rate-dependent model calibration. Quantitatively, Aqua Blue resin exhibited a higher quasi-static reference yield stress than RPG resin. The mean yield stress determined for Aqua Blue resin was $\sigma_0 = 35.67\,\text{MPa}$, whereas RPG resin reached $\sigma_0 = 23.25\,\text{MPa}$. This corresponds to an approximately 53 % higher quasi-static yield stress for Aqua Blue resin. The standard deviation bands shown in Figures 3 and 4 indicate that the scatter of the repeated quasi-static tests was limited for both materials, supporting the repeatability of the measured reference response.

The quasi-static tests therefore served two purposes: first, to compare the baseline compressive behavior of the investigated SLA-printed resins, and second, to provide the reference stress–strain response and yield stress required for the calibration of the Cowper–Symonds model.

3.2. Dynamic compression response

The dynamic compressive response obtained from the SHPB experiments is shown in Figures 5 and 6 for Aqua Blue resin and RPG resin, respectively. Both diagrams present the mean true-stress–true-strain curves for the two investigated strain-rate levels, together with the corresponding standard deviation bands. For each material, five specimens were tested at the lower and five specimens at the higher dynamic loading level. The true-stress–true-strain curves were evaluated from the measured strain-gauge signals using the same processing procedure for all experiments.

For both investigated resins, the SHPB experiments revealed a clear increase in stress level compared with the quasi-static response. The curves obtained at the higher loading level generally reached higher stress values than those measured at the lower dynamic loading level, indicating a pronounced strain-rate dependence of the compressive response of the printed photopolymer materials. The individual curves within each loading group showed comparable overall trends with a certain degree of experimental scatter between individual specimens.

The dynamic tests provided substantially higher yield stress values than the quasi-static experiments for both investigated resins. For Aqua Blue resin, the mean yield stress increased from $\sigma_0 = 35.69 \pm 2.07\,\text{MPa}$ under quasi-static loading to $112.48 \pm 5.13\,\text{MPa}$ at the lower SHPB strain-rate level and to $128.31 \pm 5.40\,\text{MPa}$ at the higher SHPB strain-rate level. The corresponding mean strain rates were $437 \pm 5\,\text{s}^{-1}$ and $1100 \pm 9\,\text{s}^{-1}$, respectively.

For RPG resin, the mean yield stress increased from $\sigma_0 = 23.25 \pm 1.37\,\text{MPa}$ under quasi-static loading to $74.54 \pm 2.18\,\text{MPa}$ at the lower SHPB strain-rate level and to $86.27 \pm 1.80\,\text{MPa}$ at the higher SHPB strain-rate level. The corresponding mean strain rates were $465 \pm 8\,\text{s}^{-1}$ and $892 \pm 14\,\text{s}^{-1}$, respectively.

Thus, both materials exhibited pronounced strain-rate strengthening. The dynamic yield stress increased by approximately 215 % and 260 % for Aqua Blue resin at the lower and higher SHPB strain-rate levels, respectively. For RPG resin, the corresponding increases were approximately 221 % and 271 %. Aqua Blue resin retained higher absolute yield stress values in all loading regimes, while RPG resin showed a comparable relative increase with strain rate.

The dynamic curves were further used to determine the yield

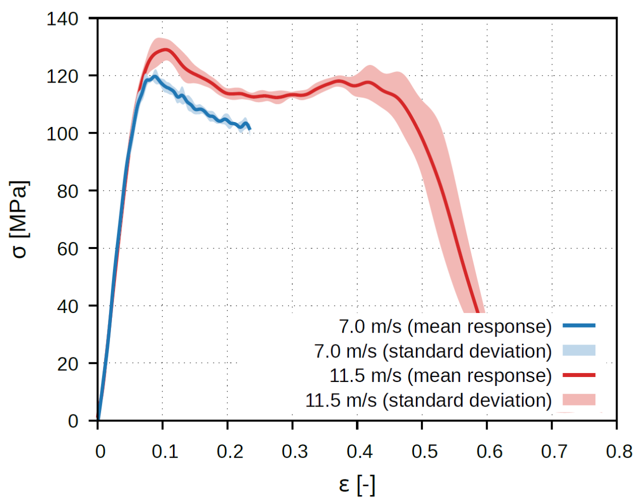

Figure 5. Dynamic response of AquaBlue resin.

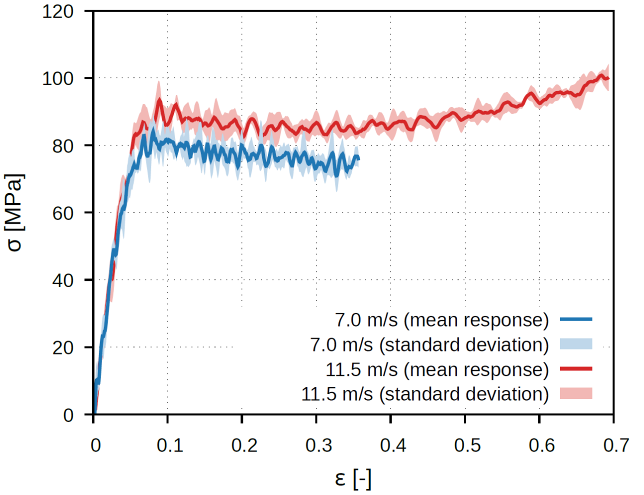

Figure 6. Dynamic response of RPG resin.

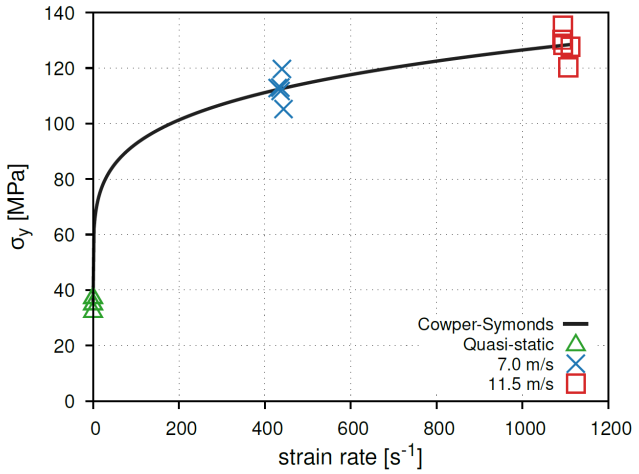

Figure 7. Cowper–Symonds model fitted to the experimentally determined yield stresses of Aqua Blue resin

stress at the corresponding strain-rate levels. These yield stress values, together with the quasi-static reference yield stresses, served as input data for the subsequent Cowper–Symonds model calibration.

3.3. Calibrated Cowper–Symonds parameters

The experimentally determined yield stress values were used to calibrate the Cowper–Symonds parameters for both investigated SLA-printed resins. For each material, the quasi-static yield stress served as the reference value σ_0, while the two SHPB loading levels provided the dynamic yield stress values at elevated strain rates. The calibration was performed independently for Aqua Blue resin and RPG resin using nonlinear least-squares fitting.

The resulting fit for Aqua Blue resin is shown in Figure 7. The experimental points show an increase of yield stress with increasing strain rate, and the fitted Cowper–Symonds curve provides a continuous engineering description of this rate-dependent strengthening. For Aqua Blue resin, the quasi-static reference yield stress was $\sigma_0 = 35.67$ MPa, and the calibrated Cowper–Symonds parameters were $C = 9.840\ \mathrm{s}^{-1}$ and $p = 4.947$. The resulting curve provides a continuous representation spanning the quasi-static reference and the dynamic yield stress levels obtained from the SHPB experiments.

The corresponding calibration for RPG resin is presented in Figure 8. Similarly to Aqua Blue resin, the RPG material exhibited strain-rate-dependent behavior, which was approximated using the same Cowper–Symonds formulation. The RPG resin exhibited a lower quasi-static reference yield stress of $\sigma_0 = 23.25$ MPa, with calibrated parameters of $C = 37.70\ \mathrm{s}^{-1}$ and $p = 3.174$. The differences between the identified parameter sets reflect the distinct strain-rate-dependent responses of the two investigated resins.

The calibrated Cowper–Symonds parameters are summarized in Table 1. Here, σ_0 denotes the quasi-static reference yield stress used to anchor the Cowper–Symonds relation, while C and p describe the strain-rate sensitivity of the material. These parameter sets provide a compact input for subsequent explicit dynamic simulations, where the quasi-static true-stress–true-strain curve can be used as the reference material response, and the flow stress is scaled according to the local strain rate.

4. DISCUSSION

The experimental results show that both investigated SLA-printed resins exhibit a clear strain-rate-dependent compressive

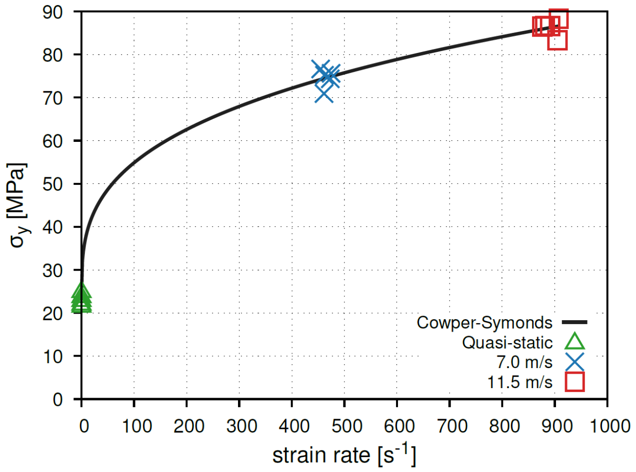

Figure 8. Cowper–Symonds model fitted to the experimentally determined yield stresses of RPG resin.

response, as quantified in Section 3 by the increase in yield stress between the quasi-static and SHPB loading regimes. The quasi-static reference yield stress was 35.67 MPa for Aqua Blue resin and 23.25 MPa for RPG resin, indicating a higher baseline compressive strength of Aqua Blue resin under the selected printing and post-processing conditions. Under SHPB loading, both materials showed a further increase in the stress level, confirming that quasi-static material data alone would not be sufficient to define material input for simulations of dynamically loaded SLA-printed structures. Although Aqua Blue resin reached higher absolute yield stress values in all loading regimes, both materials showed a comparable relative increase in yield stress under dynamic loading.

The scatter of the measured stress–strain curves within individual experimental batches was relatively small for both materials and both loading regimes, as indicated by the standard deviation bands in Figures 3-6. The RPG resin generally showed a more compact distribution of the identified yield stresses, whereas Aqua Blue resin exhibited a larger scatter in the dynamic tests. This dif-

Table 1. Calibrated Cowper–Symonds parameters for the investigated SLA-printed resins.

Material	σ_0 in MPa	C in s^{-1}	p
Aqua Blue	35.67	9.840	4.947
RPG	23.25	37.70	3.174

ference was taken into account by fitting the Cowper–Symonds parameters to all available dynamic yield-stress data rather than to a single representative point at each strain rate level.

The Cowper–Symonds model provided a straightforward engineering description of the experimentally observed increase in yield stress with strain rate. Its main advantage in the present context is the possibility of representing the rate-dependent response using only two parameters, while keeping the quasi-static stress–strain curve as the reference material input. This formulation is therefore well suited for implementation in subsequent explicit dynamic simulations of SLA-printed lattice structures, where a computationally efficient and robust representation of strain-rate dependence is advantageous.

At the same time, the calibrated curves should be interpreted with respect to the available experimental range. The calibration was based on one quasi-static loading level and two SHPB strain-rate levels. Therefore, the model provides a continuous description spanning the measured quasi-static and high-strain-rate responses, while the intermediate strain-rate region was not experimentally covered in this study. Additional tests at medium strain rates could further refine the shape of the strain-rate dependence and improve confidence in the model prediction within the transition region between quasi-static and SHPB regimes.

Consequently, the predictive capability of the calibrated parameter sets is primarily supported within the experimentally investigated strain-rate range, i.e. between the quasi-static reference response and the two SHPB strain-rate levels used in this study. Extrapolation outside this range, as well as interpolation through the experimentally uncovered intermediate strain-rate region, should therefore be treated with caution.

Another limitation is related to the phenomenological nature of the Cowper–Symonds formulation. The model captures the rate-dependent increase in flow stress, but it does not provide a comprehensive description of the rate-dependent constitutive and damage behavior of photopolymer resins. Nevertheless, for the intended use in engineering simulations of dynamically loaded printed structures, the calibrated parameter sets provide a practical and experimentally supported approximation of the strain-rate-sensitive compressive behavior of the investigated materials.

5. CONCLUSIONS

This study presented quasi-static and high-strain-rate compression testing of two commercially available SLA-printed photopolymer resins. The experiments showed a clear increase in compressive stress level with increasing strain rate for both investigated materials. The measured stress–strain curves showed satisfactory repeatability within the individual experimental batches, providing a consistent experimental basis for the subsequent material model calibration.

The experimentally determined yield stress values were used to calibrate the parameters of the Cowper–Symonds material model for each resin. The resulting parameter sets provide an engineering description of the strain-rate-dependent compressive response and are intended for future implementation in explicit dynamic simulations of SLA-printed lattice structures and mechanical metamaterials. Although the intermediate strain-rate regime remains to be experimentally characterized, the obtained results provide a practical basis for incorporating the observed rate dependence of both resins into numerical material models.

AUTHORS' CONTRIBUTION

T. Doktor: Conceptualization; Methodology; Investigation; Data curation, Writing – original raft; Writing – review & editing; **V. Drechslerová:** Design and manufacture of specimens, Writing – review & editing; **J. Falta:** Investigation, Writing – review & editing; **T. Fíla:** Data curation, Writing – review & editing; **V. Rada:** Investigation, Writing – review & editing; **B. Hora:** Investigation, Data curation, Writing – review & editing; **D. Kytýř:** Investigation, Data curation, Writing – review & editing, Funding acquisition; **P. Koudelka:** Conceptualization, Methodology, Writing – review & editing; Funding acquisition

DATA AVAILABILITY STATEMENT

Representative experimental data supporting this study are publicly available in the Zenodo repository DOI: 10.5281/zenodo.21870671.

ACKNOWLEDGEMENT

This research was supported by the Czech Science Foundation (Project No. 25-18209S), the Strategy AV21 programme "AI: Artificial Intelligence for Science and Society".

REFERENCES

[1] J. Peloquin, Y. Han, K. Gall, Printability and mechanical behavior as a function of base material, structure, and a wide range of porosities for polymer lattice structures fabricated by vat-based 3D printing, Additive Manufacturing, vol. 78, 2023, pp. 1–13. DOI: 10.1016/j.addma.2023.103892

[2] K. L. Sampson, H. Li, K. Laqua, D. Aranguren van Egmond, L. E. Dickson, J. Barroeta Robles, J. Lamouche, A. Guthrie, B. Ashrafi, S. Zou, M. Chen, J. Bell, C. Paquet, Gradient-interpenetrating polymer networks in 3d printed lattices for tunable and enhanced energy absorption, Advanced Materials Technologies, vol. 9, 2024, no. 22, pp. 1–13. DOI: 10.1002/admt.202400403

[3] A. Bustihan, I. Botiz, Recent advances in additively manufactured polymeric structures for mechanical energy absorption, Polymers, vol. 18, 2026, no. 9, pp. 1–49. DOI: 10.3390/polym18091019

[4] P. Koudelka, P. Zlámal, T. Fíla, K. Souček, V. Rada, M. Neuhäuserová, J. Šleichrt, D. Kytýř, Analysis of a 3D tetrachiral auxetic lattice under compression: Combining experimental and numerical approaches of 4D X-ray microtomography, digital volume correlation, and finite element modeling, Emergent Materials, vol. 8, Dec. 2024, no. 3, p. 2345–2364. DOI: 10.1007/s42247-024-00973-x

[5] C. Ling, A. Cernicchi, M. D. Gilchrist, P. Cardiff, Mechanical behaviour of additively-manufactured polymeric octet-truss lattice structures under quasi-static and dynamic compressive loading, Materials and Design, vol. 162, 2019, pp. 106 – 118. DOI: 10.1016/j.matdes.2018.11.035

[6] M. Kucewicz, P. Baranowski, M. Stankiewicz, M. Konarzewski, P. Płatek, J. Małachowski, Modelling and testing of 3D printed cellular structures under quasi-static and dynamic conditions, Thin-Walled Structures, vol. 145, 2019, p. 106385. DOI: 10.1016/j.tws.2019.106385

[7] F. Bandinelli, M. Scapin, L. Peroni, High strain rate testing and modeling of 3D-printed polymeric cellular structures, Thin-Walled Structures, vol. 218, 2026, p. 114081. DOI: 10.1016/j.tws.2025.114081

[8] V. Drechslerova, J. Falta, T. Fila, R. Dvorak, D. Kytyr, Effect of aging on mechanical properties of 3d printed samples using stereolitography, Acta Polytechnica CTU Proceedings, 2023, vol. 42, pp. 1 – 5. DOI: 10.14311/APP.2023.42.0001

[9] D. Miedzińska, R. Gieleta, A. Popławski, Experimental study on influence of curing time on strength behavior of sla-printed samples loaded with different strain rates, Materials, vol. 13, 2020, no. 24, pp. 1 – 16. DOI: 10.3390/ma13245825

[10] M. Shirinbayan, N. Zirak, O. Saddaoui, A. Mammeri, K. Azzouz, K. Benfriha, A. Tcharkhtchi, J. Fitoussi, Effect of build orientation and post-curing of (meth)acrylate-based photocurable resin fabricated by stereolithography on the mechanical behavior from quasi-static to high strain rate loadings, International Journal of Advanced Manufacturing Technology, vol. 123, 2022, no. 5-6, pp. 1877 – 1887.
DOI: 10.1007/s00170-022-10336-7

[11] R. Deabae, W. Herzog, A. Komeili, Rate-dependent and anisotropic mechanical behavior of elastic-50A and flexible-80A photopolymer resins, Materials Today Communications, vol. 54, 2026, p. 115492.
DOI: 10.1016/j.mtcomm.2026.115492

[12] A. Batwa, M. Daud, Y. Yang, J. Shim, Y. Li, Dynamic responses of 3-D printed polymeric materials under a wide range of strain rates, ASME International Mechanical Engineering Congress and Exposition, Proceedings (IMECE), vol. 8, 2025, pp. 1–7.
DOI: 10.1115/IMECE2025-165137

[13] S. Marais, R. Tait, T. Cloete, G. Nurick, Material testing at high strain rate using the split Hopkinson pressure bar, Latin American Journal of Solids and Structures, vol. 1, 2004, no. 3, pp. 219–339.

[14] T. Fíla, P. Zlámal, J. Falta, T. Doktor, P. Koudelka, D. Kytýř, M. Adorna, J. Luksch, M. Neuhäuserová, J. Valach, O. Jiroušek, Testing of auxetic materials using hopkinson bar and digital image correlation, EPJ Web of Conferences, 2018, vol. 183, pp. 1–6.
DOI: 10.1051/epjconf/201818302045

[15] H. Kolsky, An investigation of the mechanical properties of materials at very high rates of loading, Proceedings of the Physical Society. Section B, vol. 62, nov 1949, no. 11, pp. 676–700.
DOI: 10.1088/0370-1301/62/11/302

[16] C. Bacon, Separation of waves propagating in an elastic or viscoelastic Hopkinson pressure bar with three-dimensional effects, International Journal of Impact Engineering, vol. 22, 1999, no. 1, pp. 55 – 69.
DOI: 10.1016/S0734-743X(98)00048-7